

A Study of the Scour Characteristics and the Effects of Time on the Holes at Rectangular Pier with Semi-Circular Edges

Ibtessam Habib^{1*}, Khaled Shahot²

¹ Department of Water Resources and Environmental, College of Engineering Technology-Msallata-Libya

² Department of Civil Engineering, Faculty of Engineering, Elmergib University Khums-Libya

Abstract

This study aims to understand how scour mechanism and time affects scour depth, width, and length. The study investigates a rectangular pier model with semi-circular edges under different freestream velocities covering clear-water scour and eighty-two runs in the fluid laboratory. The flow rate ranged between 0 to 4 l/sec, the upstream water depths varied from 1.2 to 5.50 cm, and the Froude number ranged between 0.11 and 0.79. The definition of time to scour equilibrium adopted in a test is pivotal for the results of a scouring experiment since prolonged equilibrium time and experiments are essential to achieve equilibrium conditions. The temporal measurements of scour depth, d_s , were taken at $T = 20, 40, 60, 90, 120, 180, 240, 300, 360, 420,$ and 480 minutes, and the equilibrium time was when the scour hole depth remained unchanged by more than 1mm. The deepest scour in all experiments occurred upstream of the pier near the nose, and its depth increased with flow intensity. The higher Reynolds numbers gave the acceleration on the scour depth, and all models produced greater scour depths. The dimensions of the scour holes increased with higher Froude numbers for flow, where the percentage increase in the depths were 46%, 61%, 65%, and 73% for Froude numbers of 0.35, 0.4, 0.45, and 0.5, respectively, compared with $F_n=0.30$.

Keywords: Bridge piers, horseshoe vortex, equilibrium time, and rectangular pier model with semi-circular edges.

1. Introduction

The recent scour-related bridge failures worldwide attracted researchers' interest because of their grave impacts, especially their economic impacts [1] [2] [3]. Civil engineers across the globe are gravely concerned with the global scour phenomenon. Bridges on rivers or streams are vital for economic, social, and cultural development. The US has experienced over 1,000 bridge failures in the past 30 years, and 60% of them were due to scouring. Scouring is also an acute problem in some East Asian countries like Taiwan, Japan, and Korea, which experience several typhoons and flood events in the summer and autumn. Scour failures often occur unexpectedly without warning or indications of structural distress [4]. [5] reported that the 1989 catastrophic failure of several bridges on the Hatchie River in Tennessee (USA) resulted in eight fatalities. In the United States, a comprehensive study on bridge failures [6] reported that an estimate made by the Federal Highway Administration in 1978 put the damages to bridges and highways caused by each major regional flood event in 1964 and 1972 at \$100 million.

The formation of horseshoe vortices eventually produced local scours, as shown in Figure 1. The water at the upstream surface of the pier causes the flow around the pier nose to accelerate and remove the bed material from the base, especially in areas where the piers and bed materials are in contact. The water surface rises upstream of the pier to form a circular profile or a bow wave [7]. A scour hole forms when the sediment at the base region is removed at a faster rate than the rate of the sediment deposited in the base region. As the scour hole deepens, it reduces the strength of the horseshoe vortex and the rate of the sediment transported away from the base region. The scouring in a clear-water scour (a flow without bedload) decreases as the shear stress of the horseshoe vortex approaches the critical shear stress of bed particles, thus lowering the rate of transport from the base region [8] [9].

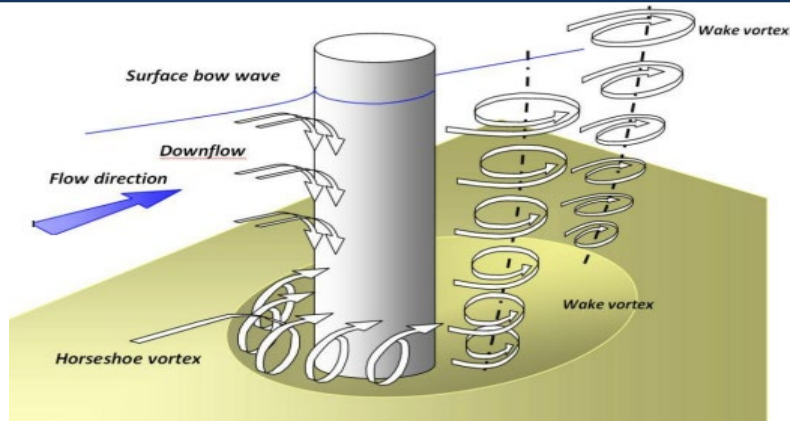


Fig 1. Illustration of a scour at a cylindrical pier [9]

Scour holes (and the maximum scour depth) begin in the homogeneous non-cohesive bed material at close to $\pm 45^\circ$ (from the midline of a circular pier) and move up to the pier nose as the scouring matures [10]. The strength of the horseshoe vortex decreases with greater scouring depth until the scour reaches an equilibrium as the shear stress due to the horseshoe vortex equals the critical shear stress of the bed material particles. The bed materials eroded from upstream and deposited some distance downstream of the pier, which resulted in the formation of a heart-shaped equilibrium scour hole, as shown in Figure 2. Maximum scouring depth is the deepest scour hole that often forms upstream of a pier.

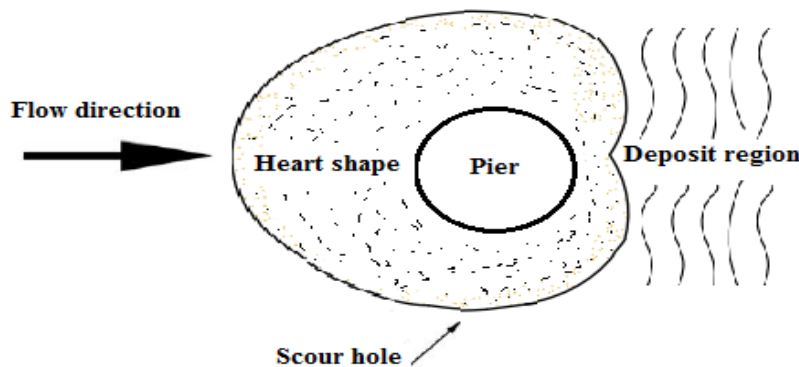


Fig 2. Schematic diagram of a heart-shaped scour hole and deposit region [11]

2. Material and Methods

2.1 Laboratory Flume

The glass fiber open flume fabricated for the experiment has steel reinforcement to provide rigidity and has a dimension of $60 \times 200 \times 570$ cm³. The diagram illustrating the experimental setup Figure 3. comprises four parts (the inlet tank, the working section, the discharge reservoir tank, and the pumping system) joined by flanged connections. The factory dispatched it as a complete assembly. A rectangular weir on the inlet tank measures the discharge in the tank. The inlet tank was filled with coarse gravel to minimize the turbulence of the incoming flow. An 8.6 cm thick sand layer was installed in the working section, with effective diameters $D_{10} = 0.26$ mm, $D_{16} = 0.29$ mm, a mean diameter of $d_{50} = 0.39$

mm, and $D_{84} = 0.50\text{mm}$. The particle size distribution has a geometric standard deviation $\sigma = D_{84}/D_{16} = 1.72$ ($\sigma > 1.3$ non-uniform sediments) for each tested model. Figure 4 presents the sieve analysis results.

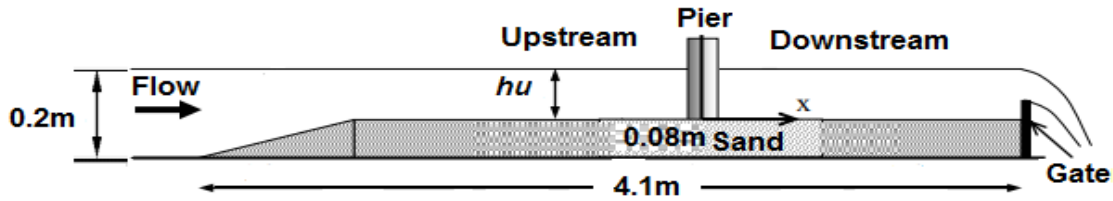


Fig 3. The experimental setup in the profile flume

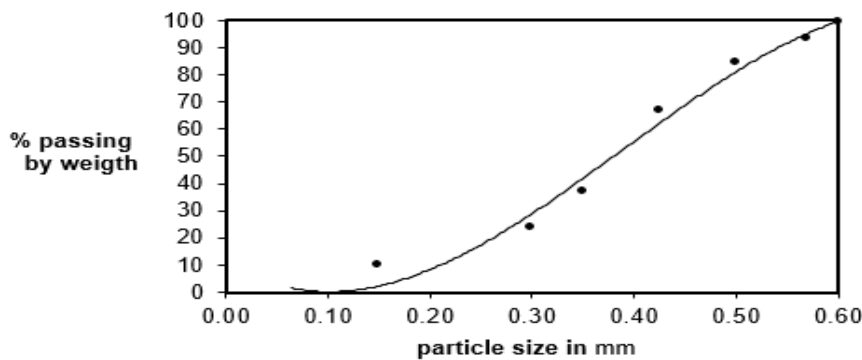


Fig 4. Bed material's grain size distribution

After installing the pier model, the sand on the bed was leveled. A rectangular pier model with a semicircular edge was fabricated from wood and coated with a plastic layer to protect it from water effects. The net dimension of the manufactured pier was 19.85 cm long, 4 cm wide (maximum width), and 20 cm high (Figure 5)). The dimensions were selected following previous studies to prevent the contraction of depth from influencing the local scour. The model width was 12% less than the flumes to prevent contraction effects, and the b/L (b is the pier width, and L is the pier length) did not exceed $1/3$ [12] [13] [14].

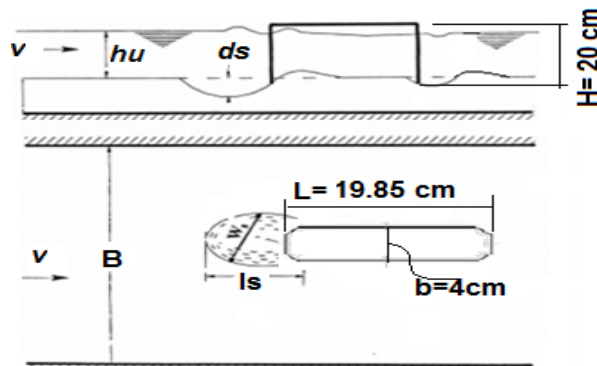


Fig 5. Schematic diagram of the tested model and the parameters measured in the experiment

2.2 Dimensional Analysis

The parameters considered in this investigation to understand the effects of scour mechanism and time on scour depth, width, and length are mean velocity (V), discharge (Q), upstream water depth (h_u), dynamic viscosity, water density, width of the main channel (B), single pier width in cm (b), median sediment grain diameter (d_{50}), and acceleration (g). Equation 1 describes the parameters

$$\frac{d_s}{b} = f\left(\frac{B}{b}, \frac{W_s}{b}, \frac{L_s}{b}, \frac{VT}{b}, \frac{d_{50}}{b}, \frac{h}{b}, d_{50}, F_n, R_n\right) \dots \dots (1)$$

Where:

$$F_n = \frac{V}{\sqrt{h_u g}}, \text{ (V is the mean velocity, and g is the gravity acceleration).}$$

$$R_n = \frac{Vb}{\nu}$$

2.3 Experimental Method

The experiments were carried out in clear water conditions and executed as follows.

1. Install the piers in the flume in the required vertical position.
2. Place the bed material (sand) with a 0.39mm mean particle size (d_{50}) in the cavity and manually level the bed with a scraper. Check the elevation of the bed surface at random points using a point gauge to ensure that the sand layer is 8.6 cm thick.
3. Gradually and carefully fill the flume with the required water depth to avoid disturbing the sediment.
4. Operate the water pump (circulation) at a low speed and gradually increase the speed to the desired flow rate to preserve the sediment. Check the tailgate to ensure the correct flow depth in the flume.
5. Monitor the testing time using a stopwatch and stop the water flow at the end of the testing time. Drain the water from the flume carefully, and record the scour's maximum depth, width, length, and location.
6. Level the sand surface (flume bed) and repeat the experiment.
7. The same steps are used to determine the effects of each study parameter (Froude number, Reynolds number, run time, scour depth, length, and width).

Table 1 summarizes the experimental parameters.

Table 1. Experimental parameters

The flow rate(Q) ranges from 0 l/sec to 4 l/sec
The upstream water depth (h_u) varies from 1.2 cm to 5.5 cm
The Froude number (F_n) during the experiment ranges from 0.11 to 0.79
Reynolds number is $31.5 \leq R_n \leq 122.03$
The temporal measurements for scour depth are (T) 20 min, 40 min, 80 min, 120 min, 180 min, 240 min, and 360 min.

3. Analysis of the results

The eighty-two experimental runs were conducted in clear water conditions to determine the effects of time on the scour hole dimensions around a rectangular pier model with semi-circular edges.

The graph in Figure (6) illustrates the association between d_s/d_{so} and T/T_o , where the scour depth reaches 90 % of the ultimate scour depth at $T/T_o = 0.50$, indicating that 90 % of the ultimate scour depth occurs at 40% of the ultimate scour depth (90% of the maximum scour depth occurs at 1.5 hours). The increase in the scour depth for ($T/T_o > 0.50$) occurs at a low rate. Equation (2) describes the relationship between d_s/d_{so} and T/T_o .

$$\frac{d_s}{d_{so}} = 10.304 \ln\left(\frac{T}{T_o}\right) + 98.609 \dots (2)$$

Where:

d_s : scour depth,

d_{so} : the ultimate scour depth.

T : run time.

T_o : time of the ultimate scour depth

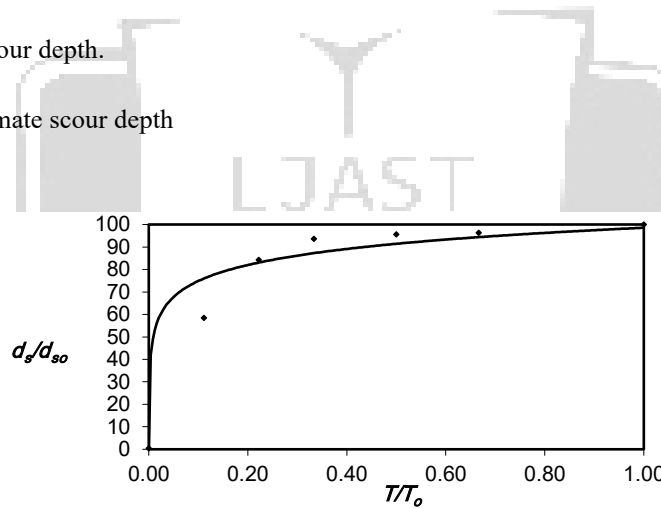


Fig. 6. Relationship between T/T_o and d_s/d_{so} at $F_n=0.44$

Figures (7) and (8) show the relationship between T/T_o and W_s/b and T/T_o and l_s/b , respectively, under flow conditions of $Q= 2.01\text{L/sec}$, $h_u = 1.80\text{cm}$, and $F_n= 0.44$ and varying durations of 20, 40, 60, 90, 120, 180, 240, and 360 min. Figure (7) shows that l_s/b is almost constant at $T/T_o > 0.65$, the relative length for a scour hole to stabilize. Equation (3) describes the relation between l_s/b and T/T_o .

$$\frac{l_s}{b} = 0.3206 \ln\left(\frac{T}{T_o}\right) + 3.0974 \dots \dots (3)$$

Where:

b : width of the pier.

l_s : length of the scour hole

Figure (8) shows that W_s/b is almost constant at $T/T_0 > 0.65$, the relative width for a scour hole to stabilize. Equation (4) describes the relation between W_s/b and T/T_0 .

$$\frac{W_s}{b} = 0.3697 \ln\left(\frac{T}{T_0}\right) + 3.604 \dots \dots (4)$$

Where:

W_s : width of the scour

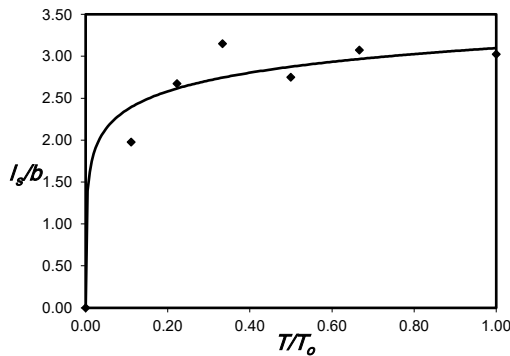


Fig. 7. Relationship between T/T_0 and l_s/b at $F_n=0.44$

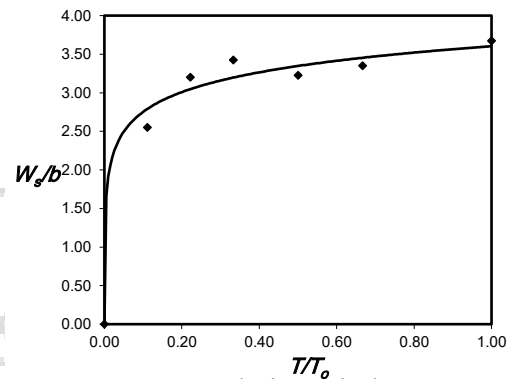


Fig 8. Relationship between T/T_0 and W_s/b at $F_n=0.44$

The measured maximum scour depths around the pier at different flow rates were plotted and used to predict the equilibrium scour depth around the round-edged rectangular pier, and the different scour hole depths are shown in Figure (9). The scour hole depths increase as the flow depth decreases, although the rate of increment is not linear. The maximum scour depth depends on time and the flow rate, where the initial depth of the scour holes increases with higher flow rates in the channel. The saturation increases with time, and the scour depth gradually reaches equilibrium.

The representative data in Figure (9) shows the association between the relative maximum scour depth ds/b and T/T_0 at different Froude numbers. It shows the gradual increase in scour depth with time at the same Froude number. The scour depth increases markedly at $T/T_0=0.33$, after which the increment is more gradual due to the fast water eddies in the first period of the scour hole formation. During this period, the sand coming out of the holes is compensated by the sand from the sides until the holes stabilize and reach equilibrium. Figure (9) shows the relative time constant at values greater than $F_n=0.30$, where the scouring depth increases significantly for the remaining Froude numbers. The higher Froude numbers indicate higher velocity and, thus, the larger vortices in front of the pier. A comparison of the curve for $F_n=0.30$ with the other curves shows that the percentage increments are 46%, 61%, 65%, and 73% for higher Froude numbers of 0.35, 0.4, 0.45, and 0.5, respectively.

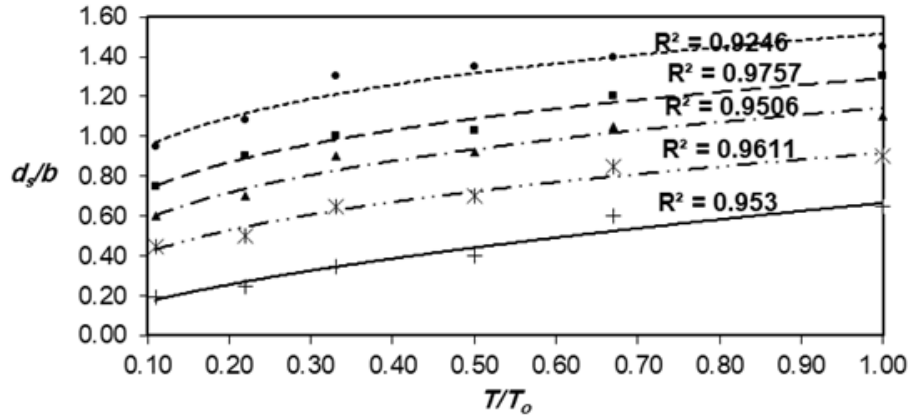


Fig 9. Effect of time on scour depth at different Fn

Figure (10) shows the largest, dimensionless scour depth against the Reynolds number for a flow discharge of 3 l/sec for a three-hour run time. The steepest gradient of the progressive scour depth occurs at the lowest Reynolds number. The increase in scour depth is minimal at high R_n , and the increase in d_s/d_{50} is 27.4% at Reynolds numbers between 70 and 110.

The flow field shows the increasing prominence of the downward flow in front of the pier and a more turbulent flow as the scour hole forms. There is a similar variation tendency in the velocities and the intensity of the turbulence in the streamwise direction in front of the pier. Generally, the Reynolds shear stress increases with the development of the scour hole, and the region with large values expands and moves upstream of the scour hole.

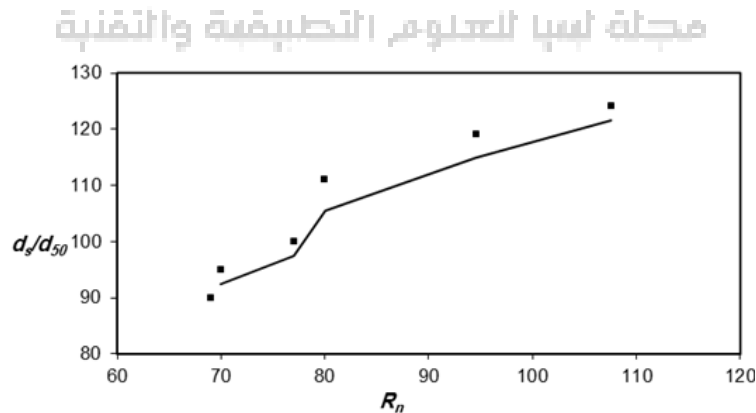


Fig 10. Relationship between d_s/d_{50} and R_n at 180 min and $Q = 3L/s$

4. Conclusions

The conclusions extracted from this research are that the deepest scours occurred upstream of the pier near the nose, and the scour depth increased with higher flow intensity. The scour depth reached the asymptote value at $T/T_o \approx 0.40$, indicating that 90% of the ultimate scour depth occurred at 40% ultimate scour depth (90% of the maximum scour depth occurred at 1.5 hours). The increment rate of scour depth for $T/T_o > 0.4$ is minimal. The data shows that the maximum scour depth could reach 70% of the pier width at about $0.5T_o$, concurring with the results of [15], which adopted a run time of three hours. The scour hole's relative length, l_s/b , and the scour's relative width, W_s/b , stabilized at $T/T_o = 0.65$. The scour hole's dimension increased with higher Froude numbers for flow, where the increase in depths were 46%, 61%, 65%, and 73% at 0.35, 0.4, 0.45, and 0.5 Froude numbers, respectively, compared to $Fn=0.30$. Finally, there was a strong reversal flow near the bed upstream of the pier and near the free surface downstream, where the negative velocity and Reynolds shear stress reduced the magnitude of the downward seepage. The sedimentation effects prevailed in the scour hole, while the erosive force was more dominant outside the scour hole. The reduced reversal flow upstream of the pier was due to the downward seepage reducing the higher order moments and turbulent kinetic energy.

References:

1. A. Johnson, A. DOCK, "Probabilistic bridge scour estimates". Journal of Hydraulic Engineering, 1998, 124.7: 750-754.
2. L. Lagasse, L. Thompson & A. Sabol, "Guarding against scour." Civil Engineering, 1995, 65.6: 56
3. S. Akib, et al, "Reducing local scouring at bridge piles using collars and geobags". The Scientific World Journal, 2014, 2014.1: 128635.
4. Y. LIN, et al, "Real-time monitoring of local scour by using fiber Bragg grating sensors". Smart materials and structures, 2005, 14.4: 664.
5. National Transportation Safety Board. Highway Accident Report. Retrieved from <http://www.nts.gov/investigations/summary/HAR900/html 1990>
6. E. ROSS et al, "Recommended procedures for the safety performance evaluation of highway features". 1993.
7. C. Grimaldi et al, "Local scouring at bridge piers and abutments: time evolution and equilibrium". In: Proc., 3rd Int. Conf. on Fluvial Hydraulics. 2006. p. 1657-1664.
8. F. Lagasse, Countermeasures to protect bridge piers from scour. Transportation Research Board, 2007.
9. V. Richardson et al, Evaluating scour at bridges. United States. Federal Highway Administration. Office of Bridge Technology, 2001.

10. I. Habib, H. Mohtar, K. Shahot, A. El-shafie, and T Sabariah, "Bridge failure prevention: An overview of self-protected pier as flow altering countermeasures for scour protection." *Civil Engineering Infrastructures Journal* 54, no. 1 2021: 1-22.
11. J. Raudkivi, R. Ettema, "Clear-water scour at cylindrical piers". *Journal of hydraulic engineering*, 1983, 109.3: 338-350.
12. W. Melville, Y. Chiew, "Time scale for local scour at bridge piers". *Journal of Hydraulic Engineering*, 1999, 125.1: 59-65.
13. W. Melville, J. Sutheri, "Design method for local scour at bridge piers". *Journal of Hydraulic Engineering*, 1988, 114.10: 1210-1226.
14. I. Habib, H. Mohtar, A. Elsaid, and A. El-Shafie, "Nose-angle bridge piers as alternative countermeasures for local scour reduction." *The Baltic Journal of Road and Bridge Engineering* 2018 13, no. 2 110-120.

